ELSEVIER

Journal of Alloys and Compounds 330–332 (2002) 307–312

Journal of ALLOYS AND COMPOUNDS

www.elsevier.com/locate/jallcom

Electronic states of hydrogen in zirconium oxide

Takanori Nishizaki[a,*], Mihoko Okui[a], Ken Kurosaki[a], Masayoshi Uno[a], Shinsuke Yamanaka[a], Kiyoko Takeda[b], Hiroyuki Anada[b]

[a]*Department of Nuclear Engineering, Graduate School of Engineering, Osaka University, Yamadaoka 2-1, Osaka 565-0871, Japan*
[b]*Sumitomo Metal Industries, Ltd., Fuso-cho, Amagasaki, Hyogo 660-0891, Japan*

Abstract

First-principles molecular orbital calculations for the electronic states of hydrogen in ZrO_2 have been carried out using the discrete variational-Xα cluster method. Both the band gap energy and the valence band structure of ZrO_2 are in good agreement with experimental results. By the introduction of a hydrogen atom, a new impurity level appears below the conduction band and the band gap is greatly reduced. Calculated partial density of states of the H 1s component in the band gap reproduces the experimental results obtained by means of Mott–Schottky analysis. The dominant chemical bond in ZrO_2 is found to be the strong ionic bond between Zr and O atoms, and the bonding character is hardly modified by the hydrogen content.

Keywords: Zirconium oxide; Hydrogen; Electronic state; DV-Xα method; XPS

1. Introduction

Zirconium alloys such as Zircaloy and Zr–Nb have been widely used as cladding materials for light water reactors (LWRs). Renewed interest in the corrosion of the cladding under the high burn-up conditions of LWRs has called for a reassessment of hydrogen behavior in the cladding. Zirconium dioxide (ZrO_2) is formed on the surface of the cladding under the corrosion process and serves as a hydrogen diffusion barrier. A sound understanding of the electronic states of hydrogen in ZrO_2 is of particular importance for minimizing the hydrogen embrittlement of the cladding.

Although several studies on the behavior of hydrogen in ZrO_2 have been carried out [1–6], there are insufficient data to elucidate the detailed electronic state of hydrogen in ZrO_2. In this work, we present first-principles molecular orbital (MO) calculations to study the electronic states of hydrogen in ZrO_2. We focus on both the energy level structure and chemical bonding character, and demonstrate how the presence of hydrogen in ZrO_2 affects the electronic states. In addition to the theoretical calculations of the quantum chemistry, the band structure of ZrO_2 was determined experimentally using X-ray photoelectron spectroscopy (XPS) measurements.

2. Experimental and computational procedures

2.1. XPS measurements

All samples used for XPS measurements were made from a commercial zirconium sheet (Nilaco) of 99.7% purity and 1.0 mm thickness. Each sample was cut into the form of a disk (about 10 mm×10 mm). A flat surface was mechanically ground and polished with abrasive paper. After mechanical treatment, it was ultrasonically degreased in acetone for 15 min. The samples were oxidized in air at 400°C for 18 h to form thin oxide films on the surface. Before the oxidation, all the samples were placed in a vacuum (~10^{-6} Torr) at 250°C for 3 h to remove gases adsorbed on the surface. All of the XPS experiments were carried out in an ultra-high vacuum (UHV) on a Quantum 2000 spectrometer (Physical Electronics). The XPS spectrum was recorded using an Al Kα (1486.6 eV) X-ray source and an analysis area of 300 μm×300 μm, with a fixed analyzer resolution of 0.25 eV.

2.2. DV-Xα cluster method

Molecular orbital calculations were performed by means of the discrete variational (DV)-Xα cluster method based on the local density function approximation. The DV-Xα method is a non-relativistic first-principles method using Slater's Xα potential as the exchange-correlation potential. Details of the DV-Xα method have been discussed at

*Corresponding author.

0925-8388/02/$ – see front matter
PII: S0925-8388(01)01447-5

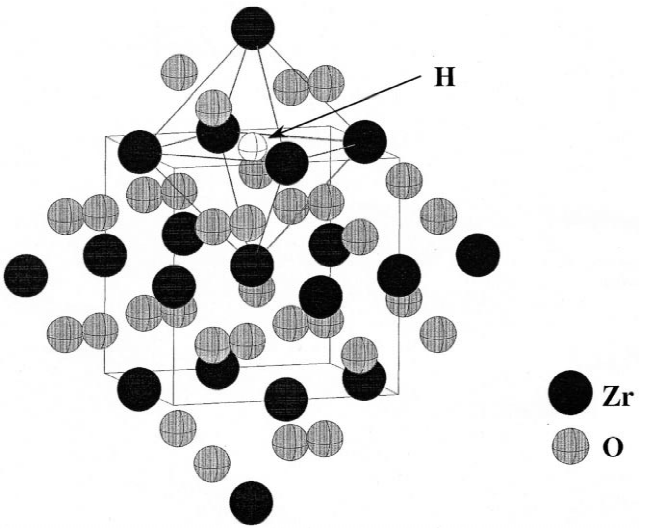

Fig. 1. Cluster model used in the calculations for hydrogen-doped $[Zr_{19}O_{32}+H]^{12+}$.

length in the literature [7–9]. Matrix elements in the secure equation were calculated by numerical, three-dimensional integration with 1000 points per atom by a random sampling method. Slater's exchange parameter, α, was fixed at 0.7 for all atoms. The basis sets of the numerical atomic orbitals used were 1s–5s, 1s–2p and 1s for Zr, O and H, respectively. One model cluster was employed, as shown in Fig. 1. The clusters belong to a tetragonal structure of space group $P4_2/nmc$ with lattice parameters of 0.36055 nm on the a-axis and 0.51797 nm on the c-axis. These lattice parameters were adopted from experimental data [10]. However, the detailed crystal structure data for hydrogen-doped ZrO_2 with tetragonal structure has not been reported. Therefore, we adopted the same lattice parameters for every cluster. The cluster used has six sites for hydrogen occupancy. In the hydrogen-doped cluster, a hydrogen atom occupies one of these sites. Each site is the central site of an octahedron, the corners of which are occupied by six Zr ions. The hydrogen content per unit cell, C_H, can be varied between 0 and 3. The formal charge was assumed to be $+4$ for all Zr ions and -2 for all O ions, but the hydrogen atom was assumed to be neutral in order to maintain a charge balance in the cluster. Therefore, the charge of every cluster was the same. The calculations were performed under no symmetry and under the condition of non-spin polarization. All clusters were embedded in a Madelung potential field.

3. Results and discussion

Figs. 2 and 3 show the energy level structures and the density of states (DOS) for $[Zr_{19}O_{32}]^{12+}$ and $[Zr_{19}O_{32}+H]^{12+}$ clusters. The discrete MO levels are broadened by the Gaussian function with a full width at half maximum (FWHM) of 0.5. In the energy level diagram, occupied and

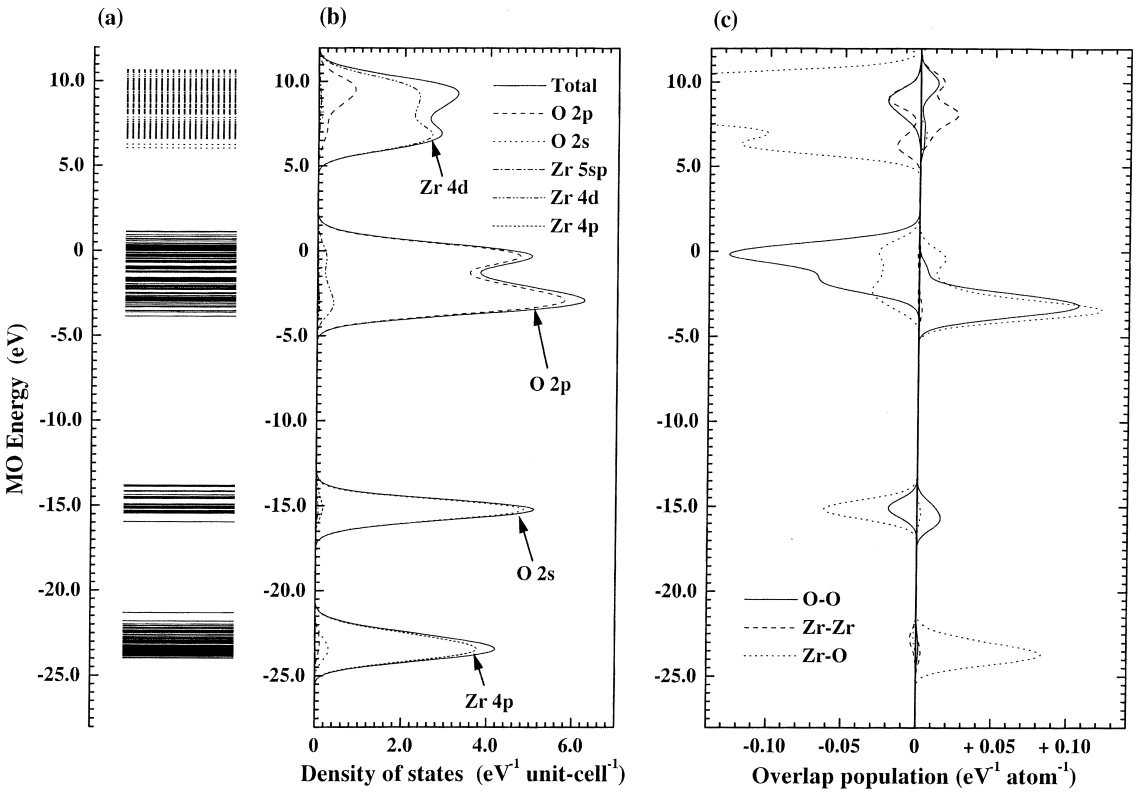

Fig. 2. (a) Energy level diagram, (b) total and partial density of states and (c) overlap population diagram for a hydrogen-free $[Zr_{19}O_{32}]^{12+}$ cluster.

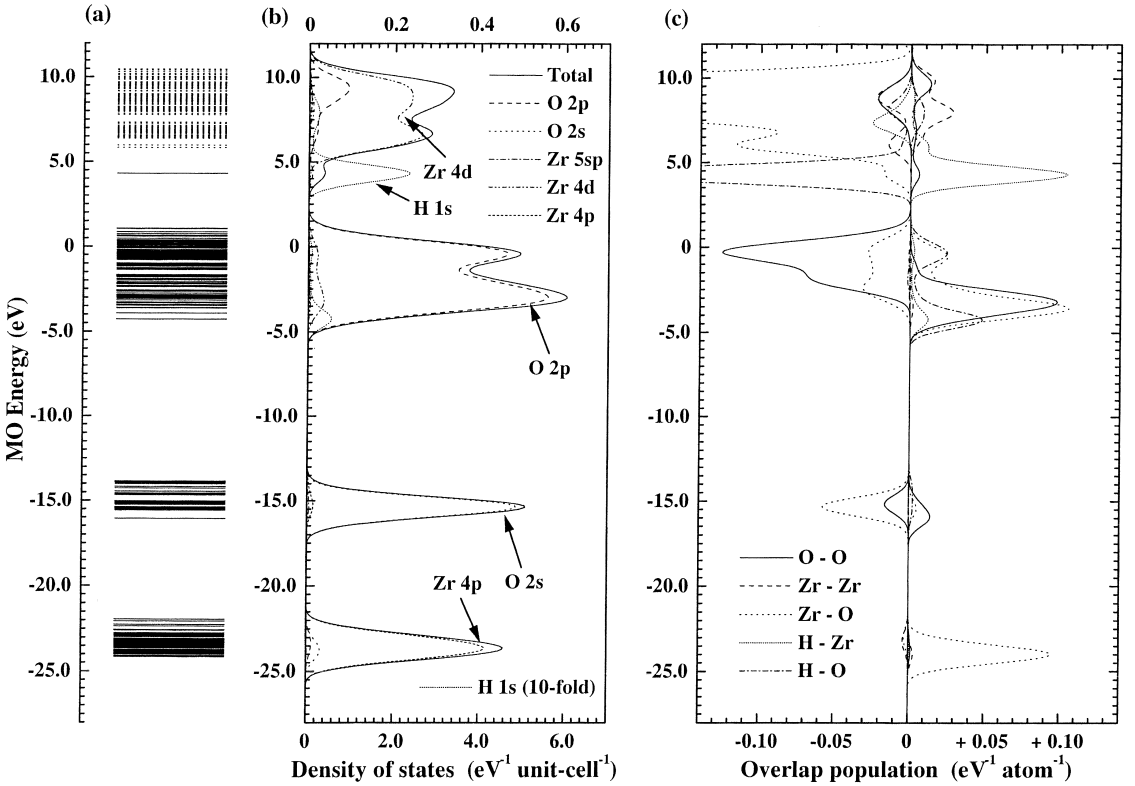

Fig. 3. (a) Energy level diagram, (b) total and partial density of states and (c) overlap population diagram for a hydrogen-doped $[Zr_{19}O_{32}+H]^{12+}$ cluster. Note the 10-fold magnification of the PDOS for the H 1s component in (b) for easy visualization.

unoccupied MO levels are indicated by solid and dotted lines, respectively. The partial density of states (PDOS) for each atomic orbital component that largely contributes to the total DOS is also plotted in the DOS diagram. In order to obtain a better understanding of the chemical bonding state, we calculated the energy distributions of overlap populations according to Mulliken's population analysis [11], as shown in Figs. 2c and 3c. The interactions between Zr–O, O–O, Zr–Zr, H–O and H–Zr in the corresponding cluster were investigated separately.

Fig. 2a and b show that the valence band is composed mainly of occupied O 2p states with a width of ~5 eV and contains small components of Zr atomic orbitals in the hydrogen-free cluster, $[Zr_{19}O_{32}]^{12+}$. The conduction band is composed primarily of unoccupied Zr 4d states with a width of ~4.5 eV. The Zr 4d band also contains a small amount of O 2p components. This indicates that there exists a weak covalent interaction between Zr and O ions. The valence band is divided into two distinct peaks. Fig. 2c shows that the lower peak is attributed to the bonding states due to the weak covalent interaction between Zr 4d and O 2p. The higher peak is of the non-bonding states, essentially composed of O 2p. The highest occupied molecular orbital (HOMO) level lies on the top of the O 2p band, and the lowest unoccupied molecular orbital (LUMO) level lies on the bottom of the Zr 4d band. The band gap between the HOMO and LUMO level is estimated at 4.9 eV. This value is in good agreement with our experimental results obtained by photoelectrochemical measurements [12] and other reports [13–16].

The valence band structure of ZrO_2 was determined experimentally using X-ray photoelectron spectroscopy (XPS). In Fig. 4 we compare the experimental spectrum with the DOS results of the cluster calculation using the hydrogen-free cluster, $[Zr_{19}O_{32}]^{12+}$. The calculated MO energy is shifted by 7 eV so as to produce the best agreement with the experimental spectrum. This discrepancy in energy levels is probably attributable to the ambiguity in the absolute energy levels that is inevitably present to some extent in DV-Xα cluster calculations due to the difference between the model clusters used and the formal stoichiometry of the corresponding compounds. However, relative values are reliable when an applicable cluster based on the actual structure is selected. The theoretical DOS reproduces the experimental XPS spectrum well. The three peaks in the spectrum are identified by our MO calculations as described above.

In the hydrogen-doped cluster shown in Fig. 3a and b, a new hydrogen-related level appears at the HOMO level between the conduction and valence bands. This impurity level is not completely filled with electrons and is composed mainly of both H 1s and O 2p orbitals. Further analysis shows that this level consists of 58.95% H 1s and 25.31% O 2p components. The H 1s component also

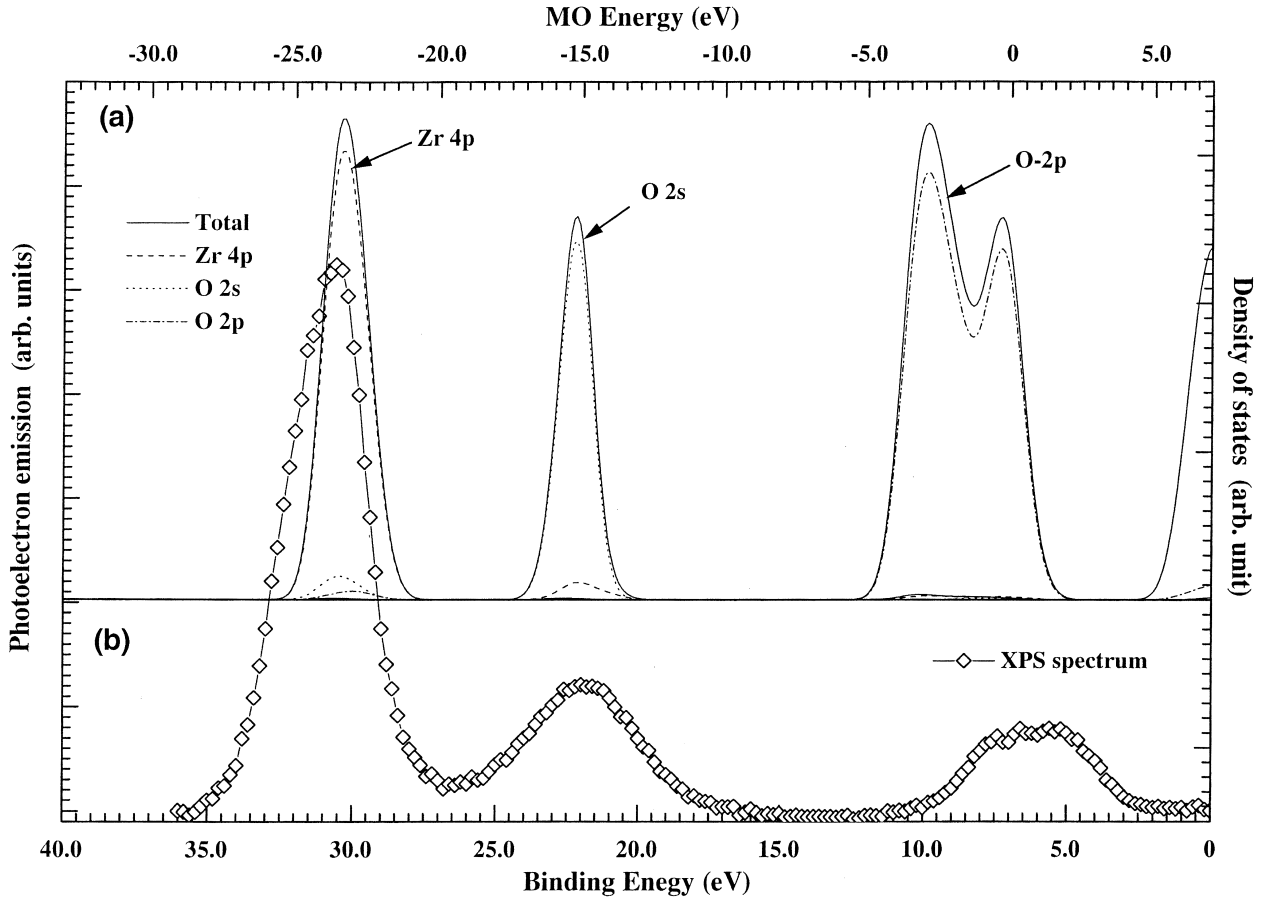

Fig. 4. Comparison between and (b) experimental XPS spectrum. Note that the DOS d e best agreement.

Fig. 4. Comparison between (a) the calculated DOS for the $[Zr_{19}O_{32}]^{12+}$ cluster and (b) the experimental XPS spectrum. Note that the DOS diagram is shifted by 7 eV so as to produce the best agreement.

appears below the valence band, where the H 1s orbital interacts with the O 2p orbital. Due to this contribution, the valence band is slightly broadened towards the lower energy side. The band gap between the HOMO and LUMO level is estimated to be 1.5 eV. This indicates that the impurity level due to a doped hydrogen atom appears in the band gap and largely reduces the band gap energy. However, except for these points, the main features of the band structures are hardly modified by the introduction of a hydrogen atom. Fig. 3c shows that bonding and anti-bonding interactions coexist between H and O atoms, while no anti-bonding contribution can be seen between H and Zr atoms. In the case of the H–O bond, a bonding interaction is dominant in the valence band, while there is an anti-bonding interaction near the HOMO level. As a result, the magnitude of the H–O covalent interaction is much smaller than that of the H–Zr interaction.

In another series of experiments [11], the distribution of the electronic states in the band gap induced by hydrogen charging was investigated by Mott–Schottky analysis. A new hydrogen-induced state was obtained in the band gap, the density being rather higher near the edge of the conduction band and decreasing towards the bottom of the band gap. The calculated partial DOS of the H 1s component in the band gap between the HOMO and LUMO level is shown in Fig. 5 together with the experimental result. The theoretical DOS agrees well with the experimental result. This indicates that hydrogen charging gives rise to a new impurity level in the band gap, which originates mainly from the H 1s component.

For a characterization of the chemical bonding, the bond order between atoms and the net charge of atoms were estimated according to the Mulliken population analysis [11]. The bond order is a measure of the strength of a covalent bond between ions. In Fig. 6 the results obtained for ZrO_2H_x ($x = 0$–3.0) are summarized in order to discuss the change in the chemical bonding with hydrogen content. The value x represents the hydrogen content per unit cell. As shown in Fig. 6a, both the O–O and Zr–Zr bond orders are negative or nearly zero for every cluster and are little changed by the hydrogen content. The Zr–O bond order is larger than any other bond. The H–O bond order increases

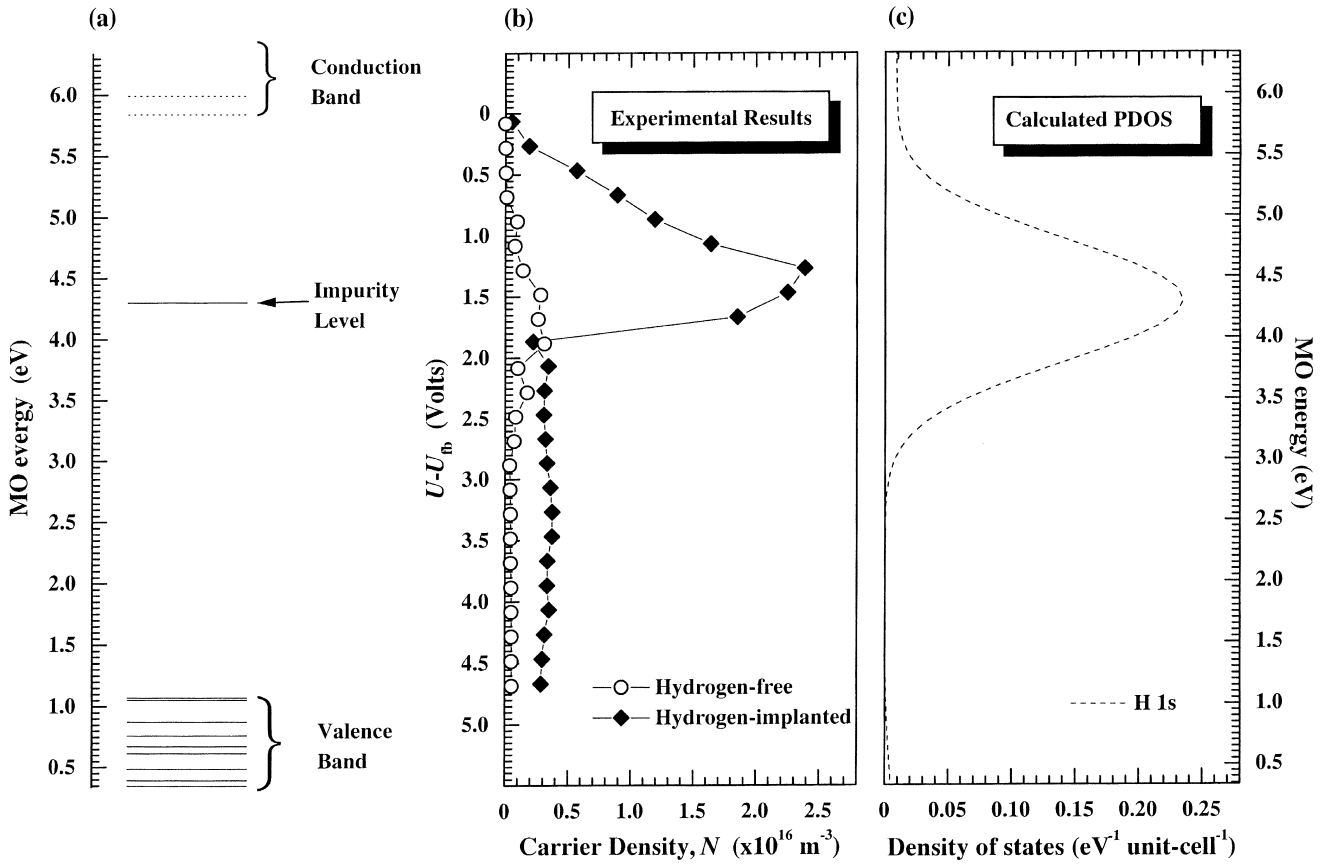

Fig. 5. Comparison of the calculated partial DOS for the H 1s component with the experimental results obtained by the Mott–Schottky analysis. (a) Energy level structures near the band gap, (b) experimental results and (c) calculated PDOS for the H 1s component.

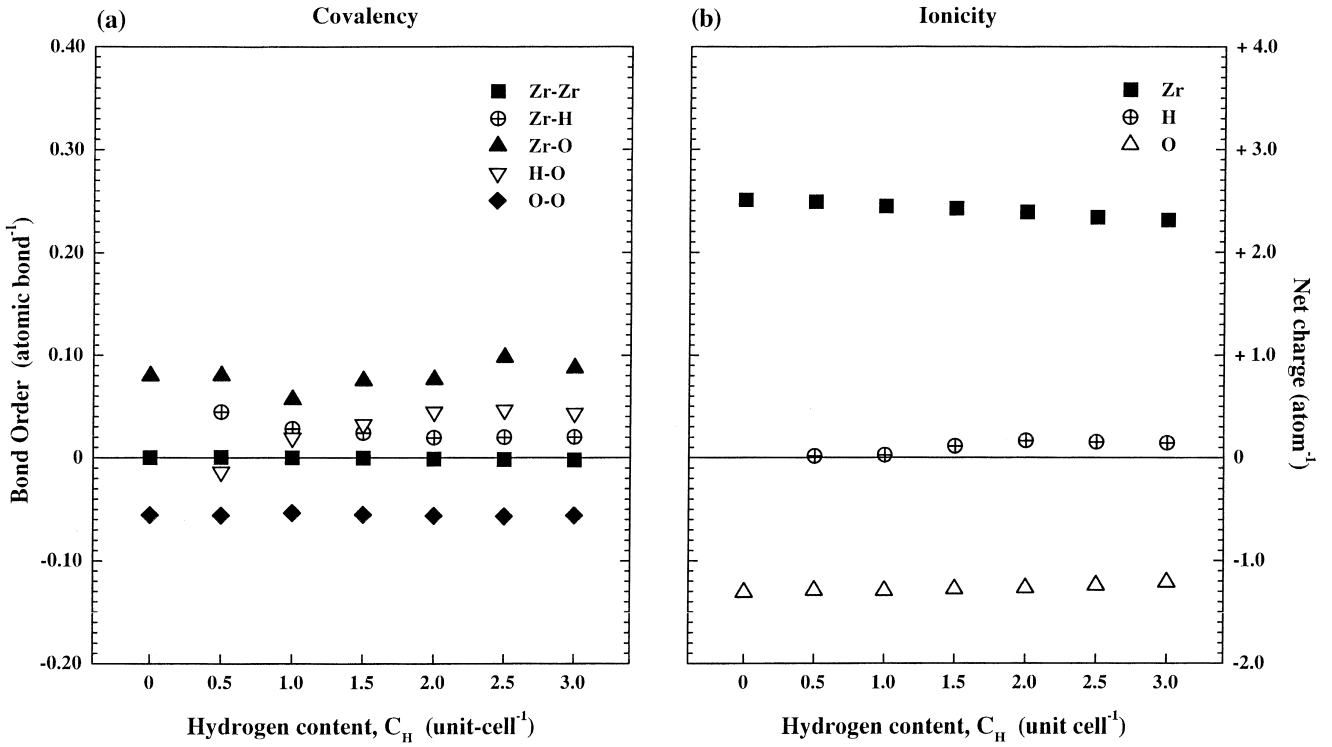

Fig. 6. Change in (a) the bond order and (b) the net charge with hydrogen content, C_H.

slightly with hydrogen content, while the Zr–H bond order decreases. The bond order of materials in which the covalent bond is dominant has been reported to be 0.2–0.5 [17–19]. This shows that all of the covalent bonds between the atoms in ZrO_2H_x are very weak and the covalent bond is not dominant in zirconium dioxides.

Fig. 6b shows the net charges of ions in the centre of the corresponding clusters. As shown in this figure, the net charges of Zr and O ions are not very sensitive to the hydrogen content and there is a strong ionic interaction between Zr and O ions. However, the ionic bonds between Zr–H and H–O ions are very week due to the small ionicity of the hydrogen atom. These results show that the ionic bond between Zr and O ions plays a major role in the bonding character of zirconium dioxide and it is hardly modified by the hydrogen content. The contribution of the ionic and covalent interaction between H and the other atoms to the bonding states in ZrO_2H_x is considerably smaller because of the small covalency and ionicity of the hydrogen atom.

4. Conclusions

We have performed first-principles MO calculations using the DV-Xα cluster method in order to investigate the modification of the electronic states of hydrogen in zirconium oxides due to the introduction of hydrogen. The band gap energy of ZrO_2, estimated to be 4.9 eV, is consistent with experimental results obtained using photoelectrochemical measurements. The valence band structure of ZrO_2 obtained by the calculation reproduces the experimental spectrum measured by X-ray photoelectron spectroscopy. The chemical bonding properties of ZrO_2 were investigated using both the density of states and the bond overlap population. The strong ionic bond between Zr and O atoms mainly contributes to the bonding states of ZrO_2 because of the small covalency between the constituent atoms. When a hydrogen atom is introduced into pure ZrO_2, a new impurity level, primarily consisting of both H 1s and O 2p orbitals, appears at the HOMO level and the band gap energy is greatly reduced to 1.5 eV. The calculated partial DOS of the H 1s component in the band gap agrees well with the experimental results obtained for hydrogen-implanted ZrO_2 by means of Mott–Schottky analysis. The bonding character of ZrO_2 is hardly modified by the hydrogen content. This suggests that no chemical bonding is formed between hydrogen and the other atoms. We conclude that the important role of hydrogen charging can be explained by the significant change in the energy level structure due to the formation of a new impurity level, resulting in reduction of the band gap energy, rather than a change in the bonding character.

Acknowledgements

The present study was partly supported by a Grant-in-Aid for Scientific Research from the Ministry of Education, Science and Culture.

References

[1] S. Yamanaka, K. Higuchi, M. Miyake, J. Alloys Comp. 231 (1995) 503.
[2] S. Yamanaka, M. Miyake, M. Katsura, J. Nucl. Mater. 247 (1997) 315.
[3] S. Yamanaka, T. Nishizaki, M. Uno, M. Katsura, J. Alloys Comp. 293–295 (1995) 38.
[4] M. Miyake, M. Uno, S. Yamanaka, J. Nucl. Mater. 270 (1999) 234.
[5] T. Nishizaki, S. Yamanaka, K. Kurosaki, K. Tateishi, M. Uno, Tech. Rep. Osaka Univ., 49, No. 2352, 1999, p. 119.
[6] D. Khatamian, J. Alloys Comp. 231 (1995) 722.
[7] J.C. Slater, Phys. Rev. 81 (1951) 385.
[8] D.E. Ellis, H. Adachi, F.W. Averill, Surf. Sci. 58 (1976) 497.
[9] H. Adachi, M. Tsukada, C. Satoko, J. Phys. Soc. Jpn. 45 (1978) 875.
[10] C.J. Howard, R.J. Hill, B.E. Reichert, Acta Crystallogr. B 44B (1988) 116.
[11] R.S. Mulliken, J. Chem. Phys. 23 (1955) 1833, 1841, 2338, 2343.
[12] M. Okui, T. Nishizaki, M. Uno, K. Kurosaki, S. Yamanaka, K. Takeda, H. Anada, in: Presented at the International Symposium on Metal Hydrogen Systems, Noosa, Queensland, Australia, 2000.
[13] P. Clechet, J. Martin, R. Oliver, C. Vallouy, C.R. Acad. Sci. Ser. C 282 (1976) 887.
[14] A.R. Newmark, U. Stimming, Langmuir 3 (1987) 905.
[15] A. Goossens, M. Vazquez, D.D. Macdonald, Electrochim. Acta 38 (1993) 1965.
[16] A. Goossens, M. Vazquez, D.D. Macdonald, Electrochim. Acta 41 (1996) 47.
[17] Y. Takahashi, H. Yukawa, M. Morinaga, J. Alloys Comp. 242 (1996) 98.
[18] Y.S. Kim, M. Mizuno, I. Tanaka, H. Adachi, Jpn. J. Appl. Phys. 37 (1998) 4878.
[19] T. Matsumura, H. Yukawa, M. Morinaga, J. Alloys Comp. 284 (1999) 82.